Original article

DOI: 10.1515/aiht-2016-67-2910

An alternative approach to studying the effects of ZnO nanoparticles in cultured human lymphocytes: combining electrochemistry and genotoxicity tests

Gina Branica[1], Marin Mladinić[2], Dario Omanović[3], and Davor Želježić[2]

Radiation Protection Unit[1], Mutagenesis Unit[2], Institute for Medical Research and Occupational Health, Division for Marine and Environmental Research, Laboratory for Physical Chemistry of Traces, Ruđer Bošković Institute[3], Zagreb, Croatia

[Received in November 2016; CrossChecked in November 2016; Accepted in December 2016]

Nanoparticle use has increased radically raising concern about possible adverse effects in humans. Zinc oxide nanoparticles (ZnO NPs) are among the most common nanomaterials in consumer and medical products. Several studies indicate problems with their safe use. The aim of our study was to see at which levels ZnO NPs start to produce adverse cytogenetic effects in human lymphocytes as an early attempt toward establishing safety limits for ZnO NP exposure in humans. We assessed the genotoxic effects of low ZnO NP concentrations (1.0, 2.5, 5, and 7.5 μg mL^{-1}) in lymphocyte cultures over 14 days of exposure. We also tested whether low and high-density lymphocytes differed in their ability to accumulate ZnO NPs in these experimental conditions. Primary DNA damage (measured with the alkaline comet assay) increased with nanoparticle concentration in unseparated and high density lymphocytes. The same happened with the fragmentation of *TP53* (measured with the comet-FISH). Nanoparticle accumulation was significant only with the two highest concentrations, regardless of lymphocyte density. High-density lymphocytes had significantly more intracellular Zn^{2+} than light-density ones. Our results suggest that exposure to ZnO NPs in concentrations above 5 μg mL^{-1} increases cytogenetic damage and intracellular Zn^{2+} levels in lymphocytes.

KEY WORDS: *comet-FISH,* in vitro*; primary DNA damage;* TP53*; voltammetry*

Nanotechnology has penetrated every segment of human life. Its ever growing presence has raised concern over the health risks it may be posing (1). The existing approaches to risk assessment have been challenged by new nanoparticles that can reach otherwise inaccessible biological structures and induce unexpected biological behaviour due to their small size and large surface area. For example, nanoparticles can both stimulate and suppress the immune system (2).

Among the most common nanomaterials in consumer and medical products are zinc oxide nanoparticles (ZnO NPs). They are widely used as drug delivery vehicles, anticancer agents, components of the restorative dental and food packaging materials, and as cosmetic, antiseptic, and ultraviolet protection products (3, 4). Exposure to ZnO NPs has come into focus with recent reports that their use may result in safety issues. Research *in vitro* has demonstrated dose-dependent cytotoxic effects of ZnO NPs in mouse neural cells, mouse ascites cells, and human epithelial lung/bronchus (5), liver (6), cardiac microvascular endothelial (7), and kidney cells (8). These toxic effects were mediated by oxidative stress and inflammation induced by ZnO NPs, which had stimulated the release of pro-inflammatory cytokines IL-6 and TNF-α.

Oxidative stress and inflammation have also been observed in animal models. Ma-Hock et al. (9) reported toxic effects of inhaled ZnO NPs on the respiratory epithelium in rats. Wang et al. (10) reported a dose-dependent increase in acute cytotoxic effects on the stomach, liver, heart, and spleen tissues of orally treated mice. Zhao et al. (11) reported ZnO NPs developmental toxicity in embryo-larval zebrafish. So far, however, safety limits for human exposure to ZnO NPs have not been proposed.

Recently, there have been attempts to assess the risk of genotoxicity posed by nanomaterials with the comet assay (12, 13). Considering that ZnO NPs have been reported to adversely affect lymphocytes (14), white blood cells seem a model of choice for testing nanoparticle genotoxicity. In our study we opted for human lymphocyte cultures to see whether 14-day exposure to increasing concentrations of ZnO NPs would produce genotoxic effects and whether they would be concentration-dependent. We also wanted to see whether lymphocytes differed in their capacity to accumulate zinc after exposure to the same concentration of ZnO NPs. To do that we took a new approach that combines voltammetry to measure intracellular exposure

Correspondence to: Gina Branica, Institute for Medical Research and Occupational Health, Ksaverska 2, 10000 Zagreb, Croatia;
E-mail: *gbranica@imi.hr*

with the methods measuring effects: the alkaline assay to determine general DNA damage and the comet-FISH assays to determine specific effects on the structural integrity and copy number of the *TP53* gene.

MATERIALS AND METHODS

By exposing lymphocyte cultures to different ZnO NP levels over 14 days we ensured that the cells would be exposed in all the phases of the cell cycle, which makes possible the direct contact between the genome and NPs. This is because certain types of NPs can interact with the DNA only during mitosis, when the nuclear membrane breaks down. Therefore, the extended exposure ensured maximum access to the genetic material (15), simulating exposure conditions *in vivo*.

We used the alkaline comet assay to determine the primary DNA damage in the lymphocytes. To identify specific effects on structural integrity and determine the number of the *TP53* gene copies and the corresponding centromeres on chromosome 17 we used the comet-fluorescence *in situ* hybridisation (comet-FISH) assay. The *TP53* gene product plays an important role in cell-cycle regulation, leading to its arrest as a response to DNA damage. Too much irreparable genome damage triggers the *TP53*-dependant pathway of apoptosis. The loss of the *TP53* gene, which is a known tumour suppressor gene, indicates increased risk of cancer development (16).

To determine ZnO accumulation we measured the effective levels of ZnO that penetrated cellular membrane by determining the levels of Zn^{2+} in treated cells with differential pulse anodic stripping voltammetry (DPASV) and high-resolution inductively coupled plasma mass spectrometry (HR-ICPMS). Anodic stripping voltammetry is the most widely used method for the estimation of metals in a variety of matrices. Its advantages are sensitivity [elements can be measured at part per trillion (ppt) concentrations], simultaneous determination of several elements, capability to distinguish between oxidation states of atomic ions, and usefulness for speciation studies (17). HR-ICPMS offers several other benefits. It is a highly sensitive method for most elements. Both major and trace elements can be detected simultaneously. HR-ICPMS can easily handle simple and complex sample matrices. It has extremely low detection limits, ranging from part per billion (ppb) to ppt. Despite the advantages of ICP sources compared to other ionisation sources, the analytical precision is limited by inherent instability of the ion signal and sample introduction devices. Instabilities may arise from either a change in energy transfer from the plasma to the sample or variation efficiency in the nebulisation and transportation of the sample (18).

ZnO nanoparticle preparation

Zinc oxide nanoparticles (ZnO NPs) with average particle size <35 nm were purchased from Sigma-Aldrich (St. Louis, MO, USA). To obtain treatment solution under aseptic conditions, the ZnO NP stock solution (50 wt. % in water) was further diluted in phosphate buffer solution (PBS), pH 7.4 (Sigma-Aldrich). Before each treatment, this solution was sonicated for 20 minutes to ensure dispersion and prevent deagglomeration and reagglomeration (19).

Blood sampling and lymphocyte collection

Peripheral blood was taken from a healthy male non-smoker donor aged 26 years with no history of chronic conditions. The blood was collected from the antecubital vein in heparin-coated vacutainers (Becton Dickenson, New Jersey, NJ, USA). We opted for the single-donor design to avoid donor variations in response and scattering of the results. The procedure was reviewed and approved by the ethics committee of the Institute for Medical Research and Occupational Health, and the donor gave his consent in writing.

Lymphocytes were isolated, and their *in vitro* cultures established following the procedure described elsewhere (20).

Culture treatment

Duplicate samples of lymphocyte cultures were incubated in a 5 % CO_2 HeraCell® 240 incubator (Kendro Laboratory Products, Vienna, Austria) at 37 °C for 14 days with solutions containing 1.0, 2.5, 5, or 7.5 μg mL^{-1} of ZnO NPs. We based this concentration choice on our preliminary experiments (data not shown). Negative control was treated with PBS. Positive control was treated with 8 μg mL^{-1} methyl methanesulphonate (MMS; Sigma-Aldrich) for the last 4 h of incubation. Figure 1 shows a detailed treatment algorithm along with the study design.

Viability testing

To determine cell viability, the lymphocytes were simultaneously stained with acridine orange and ethidium bromide (Sigma-Aldrich), 100 mg mL^{-1} of each (v/v 1:1), and analysed with a epifluorescence microscope Olympus BX 51 (Olympus, Tokyo, Japan) under 600× magnification. Hundred cells per each duplicate slide were counted to determine the percentages of viable, apoptotic, and necrotic cells (21).

Experimental design

We took two routes to assess primary DNA damage (Figure 1). The first was to collect the entire lymphocyte culture population treated with ZnO NPs on the 15th day. The cultures were centrifuged at 300 *g* for 5 min, and the cells washed twice in a fresh culture medium (RPMI 1640, Gibco, Paisley, UK). The resulting lymphocyte pellet was

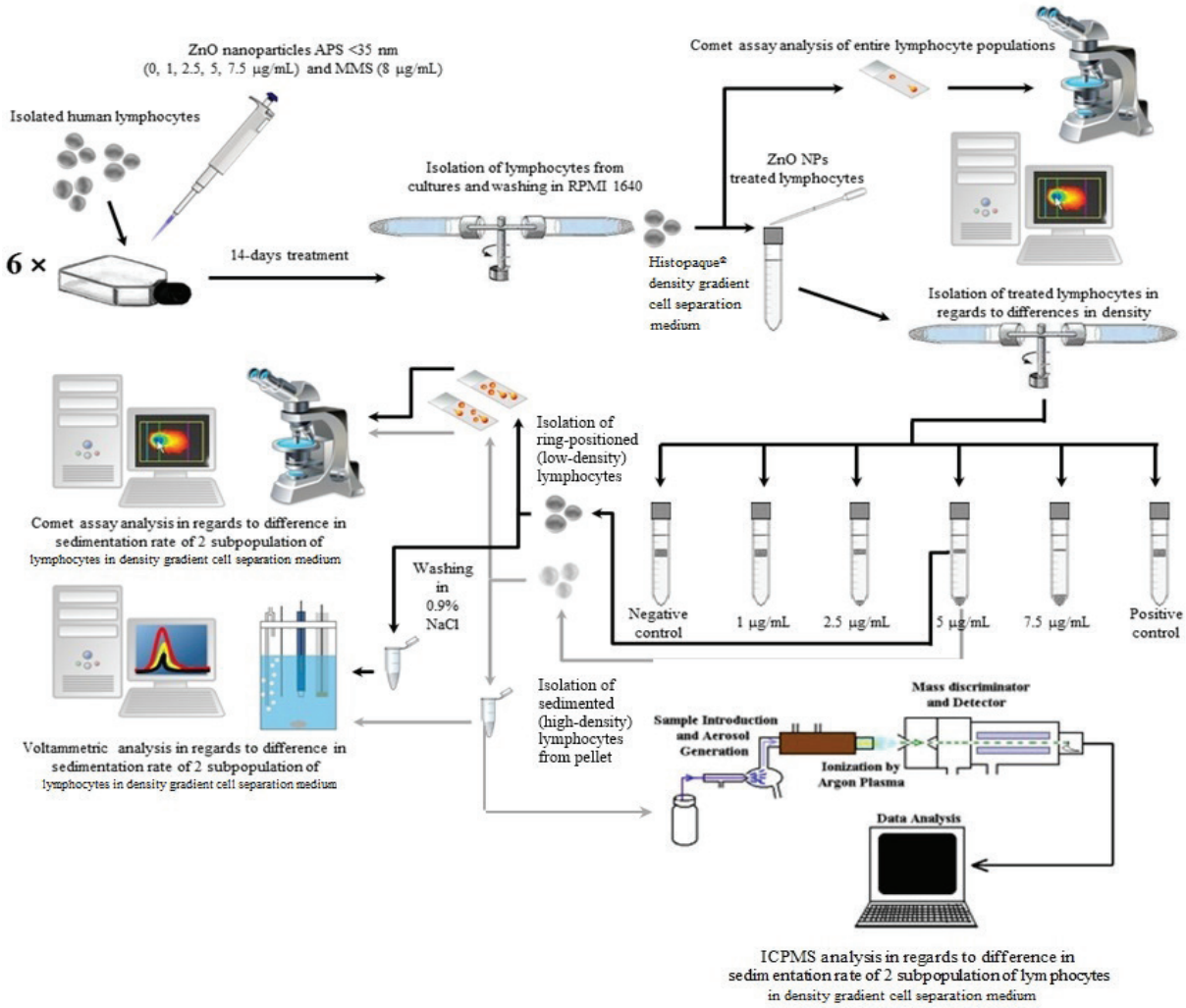

Figure 1 *Scheme of the experimental design*

diluted in saline (0.3 mL; 0.9 % NaCl w/w) and cell density determined. One microlitre of suspension containing 10^4 lymphocytes was mixed with 100 μL of 0.5 % low melting point agarose (Sigma-Aldrich) and placed on a precoated slide to prepare the microgels for the alkaline comet assay.

The second route was to collect lymphocyte cultures on day 15 (as in the first), centrifuge them at 300 *g* for 5 min, wash once and resuspend in RPMI 1640 (3 mL), layer on the Histopaque® 1077 reagent (3 mL, Sigma-Aldrich), and centrifuge at 400 *g* for 30 min to isolate lymphocytes. Isolation resulted in the separation of two lymphocyte populations. The low-density population formed a ring in the isolation medium, while the high-density population pelleted at the bottom of the tube (Figure 1). Each population was extracted separately, washed twice in RPMI 1640, and diluted in saline (0.3 mL). The slides for the comet assay were prepared according to the standard procedure (22). For each ZnO NP concentration tested, as well as for negative and positive controls we prepared four slides. Two were used for the alkaline comet assay and the other two for the comet-FISH assay.

Alkaline comet assay

For the alkaline comet assay we followed the procedure described by Singh et al. (22) with minor modifications. After a 15-minute denaturation followed electrophoresis at 0.7 V cm^{-1} and 300 mA for another 15 min. After electrophoresis, the slides were neutralised and stained with ethidium bromide. Scoring included 100 comets per each duplicate slide using the Comet Assay IV image analysis system (Perceptive Instruments, Suffolk, UK) coupled with epifluorescence microscope (Olympus BX 51) under 200× magnification. We looked for tail length and the percentage of DNA in tail (tail intensity) as the main DNA damage parameters.

Comet-FISH assay

The slides for the comet-FISH assay were processed according to the protocol described by Mladinić and Želježić (23). After electrophoresis and neutralisation, the slides were dehydrated in an ethanol series (70-100 %) and air dried. For each treatment we analysed 30 cells on each of the two duplicate slides using an Olympus AX70

epifluorescence microscope and CytoVision FISH software (Applied Imaging, Dornach, Germany). We recorded the position of the signals for the *TP53* gene and cen 17 in nucleoids and the number of copies. Then we scored the number of signals in the comet tail and head. The absence of the signals from both tail and head was considered a loss of heterozygosity (20).

DPASV and HR-ICPMS analysis of lymphocyte Zn^{2+} concentration

All chemicals used for the preparation of the samples were of high purity: ASTM type I ultra-pure water (Milli-Q; 18.2 MΩ cm, Millipore/Merck, Darmstadt, Germany), Trace SELECT® concentrated HNO_3 (Fluka, Milan, Italy), and sodium-acetate (NaAc; Merck). Aliquots of lymphocytes obtained as described above (Figure 1) were washed two more times in saline, centrifuged at 300 g for 5 min, and the pellet was resuspended in saline to obtain the final cell concentration of 10^5 cells mL^{-1}. Lymphocyte suspension (15 mL) was acidified with ultra-pure HNO_3 (150 µL; Trace SELECT®, Fluka) and left to rest overnight. The samples were then transferred to fluorinated ethylene propylene (FEP) bottles and UV-irradiated under a 250 W high-pressure Hg-lamp for another 24 h for the organic matter to decompose and transform all dissolved Zn into a specimen that can be measured with DPASV. As the working volume of the electrochemical cell used in DPASV is 15 mL, we needed to dilute the sample (~15 mL), so that it would not be used up for one analysis. The solution for the measurement was prepared by taking an aliquot of undiluted primary sample, adding 0.5 mL of 4 mol L^{-1} NaAc) to adjust pH around 4, and adding Milli-Q water to fill up the 15 mL volume. The blank sample containing HNO_3, NaAc, and Milli-Q water used for sample preparation was measured separately and found to contain 0.11 ng mL^{-1} of Zn^{2+}, most of which came from Milli-Q water. We therefore corrected our Zn^{2+} measurements in treated/control samples for the blank measurement, as we followed the same dilution procedure for all samples.

The concentration of Zn^{2+} was measured with DPASV as described by Vukosav et al. (24). Accumulation time was 1 min, and accumulation potential was -1.2 V. Figure 2 shows a typical set of the obtained voltammograms and the corresponding calibration plot (inset). For the measurement signal we used the peak Zn^{2+} voltammogram that we transformed using the 2nd derivative transformation (25). For Zn^{2+}control measurements we used the semi-quantitative HR-ICPMS (Element 2, Thermo Fisher Scientific, Bremen, Germany) (26).

Statistical analysis

Prior to statistical analysis we normalised all data ranges using base 10 log transformation. Differences in comet assay parameters and Zn^{2+} concentrations in lymphocytes were tested with the one-way ANOVA. The same method was used for low- and high-density lymphocytes. We also used the one-way ANOVA to test the differences in measured Zn^{2+} concentrations between DPASV and HR-ICPMS. To test the dependence of each cytogenetic endpoint on intracellular Zn^{2+} concentration and on ZnO concentration used in the treatment we used regression analysis. This method was also used to assess the correlation between the treatment ZnO NP concentrations and intracellular Zn^{2+} concentrations (determined with DPASV). All analyses were run on Statistica 12.0 software (StatSoft, Tulsa, OK, USA).

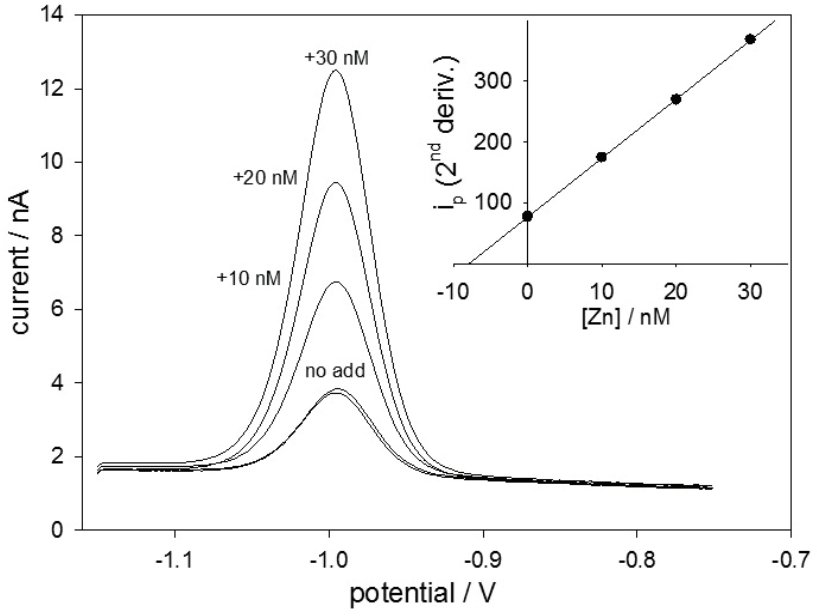

Figure 2 *Typical DPAS voltammograms of Zn^{2+} levels following the Tube 2,5, 5x standard addition method with a threefold dilution. Inset: standard addition plot from which Zn concentration was determined*

RESULTS

Zinc concentrations in treated lymphocytes

The 14-day treatment of lymphocyte cultures with ZnO NPs in the concentrations of 2.5, 5, and 7.5 μg mL^{-1} resulted in the separation of the lymphocytes into two populations of cells according to their relative density (Figure 3). Low-density lymphocytes formed a ring in Histopaque®, while high-density cells settled at the bottom, forming a pellet. This separation was not observed at ZnO NP concentration of 1 μg mL^{-1} or in negative control samples, all of which formed a ring. Even though the separation started with 2.5 μg mL^{-1}, the differences in intracellular Zn^{2+} concentrations between high-density cells and negative control or low-density cells were not significant (37.2±0.0 ng 10^{-5} cells *vs.* 13.8±4.9 ng 10^{-5} cells or *vs.* 19.5±1.7 ng 10^{-5} cells, respectively).

The accumulation of intracellular Zn^{2+} became significant with exposure to 5.0 and 7.5 μg mL^{-1} of ZnO NPs. In low-density lymphocytes it was significantly higher than in negative control (47.1±1.4 and 149.2±7.3 ng 10^{-5} cells, respectively), and in high-density lymphocytes it was significantly higher than in both negative control and low-density lymphocytes (207.2±3.4 and 430.2±8.1 ng 10^{-5} cells, respectively).

Both DPASV and HR-ICPMS used for the determination of intracellular Zn^{2+} levels showed very consistent and reproducible results over the entire range of concentrations and their values did not significantly differ (Figure 4). However, we considered the DPASV results more accurate.

Regression analysis showed a significant correlation between the applied ZnO NP concentrations and DPASV intracellular Zn^{2+} measurements.

Cell viability

Significant differences in the number of apoptotic cells started to show at 5 μg mL^{-1}, but only between high-density and negative control lymphocytes. This difference increased at 7.5 μg mL^{-1} and also became significant between high-density and low-density lymphocytes (Table 1).

Alkaline comet assay

We found no significant differences in the tail length and intensity between the unseparated ZnO NP-treated and negative control cells (first route; Table 2). In the separated cells, similar results were observed for low-density lymphocytes, except for tail intensity in the cells treated with 5 μg mL^{-1} of ZnO NPs, which increased significantly. High-density lymphocytes treated with the highest concentrations of ZnO NPs (5 and 7.5 μg mL^{-1}) had significantly greater tail length and intensity than negative control. Similar was the difference from low-density lymphocytes at 5 μg mL^{-1}, except for the tail length (Table 2).

Regression analysis showed a significant correlation between both the ZnO NP and Zn^{2+} concentrations and the comet tail length.

Comet-FISH analysis

Table 3 shows the fragmentation and deletion rate of the *TP53* gene and the corresponding chromosome 17 centromere. In the unseparated lymphocytes, a significant increase in *TP53* fragmentation was observed in samples treated with 2.5, 5, and 7.5 μg mL^{-1} of ZnO NPs compared to negative controls. ZnO NP treatment did not cause the loss of *TP53* heterozygosity.

In low-density lymphocytes significant *TP53* fragmentation was detected only in the sample exposed to 7.5 μg mL^{-1} of ZnO NPs.

The structural integrity of the *TP53* gene was more impaired in the high-density lymphocytes. Treatment with ZnO NPs concentrations of 2.5, 5, and 7.5 μg mL^{-1} resulted in significantly higher occurrence of *TP53* signals in the comet tail compared to negative controls. Fragmentation rates in high-density lymphocytes exposed to 2.5 and 5 μg mL^{-1} were also significantly higher than in low-density lymphocytes. The percentage of the fragmented centromere 17 copies in high-density cells became significantly higher only at 5 μg mL^{-1} but not at 7.5 μg mL^{-1}. We observed no significant differences in the deletion of the *TP53* copies between the treated and untreated or high and low-density groups.

Regression analysis showed a significant correlation between both the ZnO NP and Zn^{2+} concentrations and impaired structural integrity of the *TP53* gene (Table 3).

DISCUSSION

Our study is the first to investigate nanoparticle genotoxicity in lymphocyte populations separated by density due to different uptake of ZnO NPs. Unlike earlier studies (15, 27, 28), which used whole lymphocyte populations, ours is a novel approach that compares the effects of ZnO NPs by combining DPASV and HR-ICPMS with two comet assays.

The added value of our study was the testing of extended-term lymphocyte cultures instead of acute testing. By implementing this approach we ensured that the cells were exposed to ZnO NPs throughout the cell cycle, which makes possible the direct contact between genome and NPs.

Extended exposure to ZnO NPs led to significantly different results between the two approaches. When the unseparated lymphocytes were evaluated for viability, we found no significant differences between the treated and control cells, regardless of the concentration used (Table 1), but in the separated populations these differences became significant at concentrations above 5 μg mL^{-1}, and the proportion of apoptotic cells was significantly higher in high-density lymphocytes.

Table1 *Results of ethidium bromide/acridine orange staining of lymphocyte cultures treated with ZnO NPs for 14 days*

After-treatment procedure	ZnO treatment (μg mL^{-1})	Viable	Apoptotic (mean %±SD)	Necrotic
Unseparated lymphocytes	1	91.5±3.5	8.0±2.8	0.5±0.7
	2.5	90.0±1.4	8.5±2.1	1.5±0.7
	5	92.5±0.7	7.0±1.4	0.5±0.7
	7.5	88.0±2.8	8.5±2.1	3.5±0.7
	Negative control	93.0±1.4	7.0±1.4	0.0±0.0
	Positive control	74.6±5.1[1]	19.5±3.4[1]	5.9±1.7
Low-density lymphocytes separated in Histopaque®	1	88.5±0.7	11.5±0.7	0.0±0.0
	2.5	91.0±1.4	7.5±0.7	1.5±0.7
	5	89.0±1.4	10.0±2.8	1.0±1.4
	7.5	90.0±4.2	8.0±4.2	2.0±0.0
	Negative control	91.5±2.1	8.0±1.4	0.5±0.7
	Positive control	73.4±2.1[1]	21.9±4.0[1]	4.7±0.8
High-density lymphocytes separated in Histopaque®	1	-	-	-
	2.5	87.5±0.7	8.5±3.5	4.5±2.1
	5	82.0±1.4[1]	16.0±1.4[1]	2.0±0.0
	7.5	76.5±2.1[1,2]	20.0±7.1[1,2]	3.5±4.9
	Negative control	-	-	-
	Positive control	-	-	-

[1]statistically significant compared to negative control; [2]statistically significant compared to low-density cells. Null values mean that there were no high-density cells in the isolation medium, only low-density ones

Table 2 *Results of the alkaline comet assay in lymphocyte cultures treated with ZnO NPs for 14 days*

After-treatment procedure	ZnO treatment (μg mL^{-1})	Tail length (μm, mean±SD)	Tail intensity (% DNA, mean±SD)
Unseparated lymphocytes	1	23.7±5.1	2.6±6.0
	2.5	23.9±3.6	2.1±5.1
	5	23.9±4.4	3.4±6.6
	7.5	23.1±1.7	3.9±3.1
	Negative control	24.5±1.9	0.9±1.2
	Positive control	34.7±12.0[1]	10.6±4.9[1]
Low-density lymphocytes separated in Histopaque®	1	25.4±6.3	2.6±6.0
	2.5	26.3±3.1	0.9±1.2
	5	26.7±7.4	3.9±12.7[1]
	7.5	25.9±5.1	3.4±3.4
	Negative control	26.2±2.4	0.9±1.2
	Positive control	36.0±14.2[1]	12.7±4.6[1]
High-density lymphocytes separated in Histopaque®	1	-	-
	2.5	26.8±8.9	3.0±6.2
	5	39.4±26.3[1,2]	17.7±27.4[1]
	7.5	38.4±21.9[1,2]	10.7±16.4[1,2]
	Negative control	-	-
	Positive control	-	-

[1]statistically significant compared to negative control; [2]statistically significant compared to low-density cells. Null values mean that there were no high-density cells in the isolation medium, only low-density ones

Using DPASV and HR-ICPMS we clearly established that intracellular Zn^{2+} content in high-density cells was significantly higher than in both negative control and low-density cells exposed to the same ZnO NP concentrations (Figure 3) and that higher accumulation of Zn^{2+} triggered a greater cytotoxic effect. These findings correspond to the observations reviewed by Ivask et al. (27). Kim et al. (28) reported that ZnO NPs hindered mitochondrial function in rat alveolar epithelial cells *in vitro* by impairing transmembrane electron transport through increased inner membrane permeability. They also suggested that it was Zn^{+2} released from nanoparticles that contributed to the induction of oxidative stress. Sharma et al. (6) also proposed extensive reactive oxygen species formation as a contributor to apoptosis in a HepG2 cell line exposed to ZnO nanoparticles for 12 h. The exact mechanism of ZnO cytotoxicity, however, remains to be determined. Guo et al. (29) suggest that ZnO NPs trigger cell death by activating caspase-12 and by reducing the levels of caspase-9 and bcl-2 at the same time.

Differences in the observed ZnO NP cytotoxicity between our two approaches could be attributed to the composition of the lymphocyte suspensions used for viability testing. The lymphocyte population used in the first approach (without separation) contained cells which took up different amounts of ZnO NPs. Another important factor which might significantly affect both cyto- and genotoxicity findings are the intracellular concentrations of Zn^{2+} ions released from NPs. They might also vary between single cells, which further complicates the interpretation of our results.

Nevertheless, if the interpretation of the results were based only on the first approach, this could lead to a wrong conclusion, as no one could estimate the ratios between high and low-density cells or the extent of the oxidative stress which might have been caused by Zn^{2+} accumulation in individual cells. In other words, our results in these mixed populations might underestimate the real cyto- or genotoxicity caused by the treatment.

The advantage of the second approach (with separation) allowed us to distinguish between low-density lymphocytes, which exhibited lower cytotoxicity and accumulated lower amounts of ZnO and high-density ones.

Regardless of the separation, our study has shown that a significant increase in primary DNA damage started with exposure to 5 μg mL^{-1} of ZnO NPs (Table 1). Mu et al. (30) provided evidence on Zn release from ZnO NPs administered in the concentrations below 5.5 μg mL^{-1}. The level of dissolution they observed correlated with genome damage induced in different epithelial cell lines measured with the alkaline comet assay. Similar results have been reported by Demir et al. (31) for ZnO NPs of 50-80 nm in diameter. They detected genotoxic effects (specifically, oxidised bases in DNA) in human embryonic kidney fibroblasts and mouse embryonic fibroblasts at concentrations above 10 μg mL^{-1}. Zinc oxide NPs are capable of inducing primary DNA damage in many other human cell models *in vitro*: human epidermal cells (32), cervix carcinoma Hep-2 cells (33), bronchial epithelial BEAS-2B cells (34), epidermal keratinocytes (35), nasal mucosa cells (36), liver HepG2 cells (37), and hepatocytes (38). All these models showed dose-related effects on comet assay parameters. Our study confirms this dose-response relationship: tail length significantly correlated with ZnO NPs concentrations and intercellular Zn^{2+} concentrations. The difference, however, is that the cited studies evaluated genome damage induced by acute exposure, while ours measured the effects of longer-term exposure in lymphocytes separated by density,

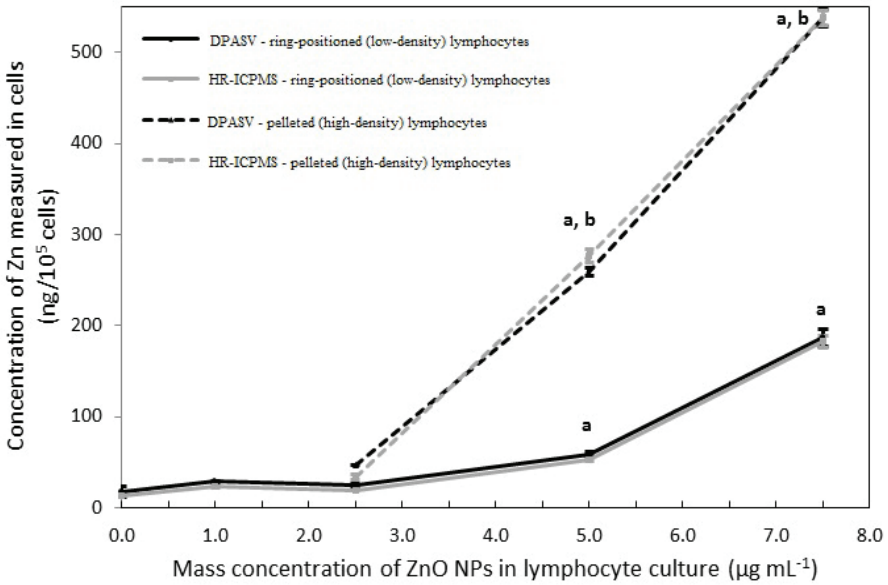

Figure 3 *Average Zn^{2+} concentrations in lymphocyte cultures treated with ZnO NPs for 14 days determined with the differential pulse anodic stripping voltammetry (DPASV) and high resolution inductively plasma mass spectrometry (HR-ICPMS).[a]significantly different from negative control; [b] significantly different from low-density lymphocytes ($p<0.05$)*

Table 3 *Comet-FISH assay-determined fragmentation and deletion of the TP53 gene and centromere of chromosome 17 in lymphocyte cultures treated with ZnO nanoparticles for 14 days*

After-treatment procedure	ZnO treatment (μg mL^{-1})	Fragmented copies		Deleted copies	
		TP53 gene	Cen 17	TP53 gene	Cen 17
		(mean %±SD)	(mean %±SD)	(mean %±SD)	(mean %±SD)
Unseparated lymphocytes	1	21.5±11.8	3.4±4.7	3.3±0.0	3.4±2.3
	2.5	36.6±4.7[1]	27.5±3.5[1]	4.2±1.2	0.0±0.0
	5	40.0±4.7[1]	21.6±2.3	3.8±0.6	0.8±1.2
	7.5	35.0±7.1[1]	13.4±9.4	4.2±1.2	1.7±0.0
	Negative control	13.3±0.0	5.0±2.4	2.5±1.1	0.8±1.2
	Positive control	49.7±8.5[1]	22.1±3.6[1]	10.3±3.6[1]	5.0±2.1[1]
Low-density lymphocytes separated in Histopaque®	1	15.0±2.4	3.3±4.7	3.3±0.0	3.3±2.3
	2.5	18.3±2.4	11.7±7.1	5.0±2.4	1.7±2.4
	5	20.0±4.7	16.7±0.0	5.0±2.4	2.5±3.5
	7.5	35.0±7.1[1]	18.3±2.4	6.7±0.0	2.5±1.2
	Negative control	13.3±0.0	5.0±2.4	2.5±1.1	0.8±1.2
	Positive control	48.1±6.2[1]	25.2±6.9[1]	8.0±2.6	4.6±2.0
High-density lymphocytes separated in Histopaque®	1	-	-	-	-
	2.5	38.3±11.8[1,2]	18.3±2.4	5.8±1.2	2.5±3.5
	5	48.3±2.4[1,2]	25.0±11.8[1]	5.0±0.0	3.3±0.0
	7.5	48.3±2.4[1]	21.7±2.4	5.8±1.8	3.3±4.7
	Negative control	-	-	-	-
	Positive control	-	-	-	-

[1]statistically significant compared to negative control; [2]statistically significant compared to low-density cells. Null values mean that there were no high-density cells in the isolation medium, only low-density ones

most likely due to different ZnO NPs uptake. In addition, the comet-FISH assay has revealed that ZnO NPs at concentrations above 2.5 μg mL^{-1} are capable of compromising primary DNA integrity (Table 3) in an intracellular concentration-dependent manner. The presence of ZnO NPs in cells may impair *TP53* transcription. This impairment makes the cells more susceptible to genotoxic effect (39).

We found a significant correlation between *TP53* fragmentation (primary damage) and both intracellular Zn^{2+} concentration and general primary DNA damage. It seems that the genotoxic action of ZnO NPs *per se* or via ROS induction randomly targets various genome regions rather than specific sites.

Genome integrity, and therefore functionality, was significantly affected by ZnO NPs in a concentration-dependent manner. This dependence, however, was not clear between the loss of *TP53* copies loss and the applied ZnO or intracellular Zn^{2+} concentrations.

Considering that the frequency of *TP53* deletions showed a limited and insignificant correlation with the frequency of *TP53* fragmentation, it is possible that the damage accumulated in the gene locus may be related to a later loss of gene copies, but this has to be studied further. This also suggests that gene fragmentation rate may be considered as a biomarker of exposure, while the deletion frequency should rather be considered as a biomarker of effect. Together with previous report by Ng et al. (40), who claim that an effective response to the genotoxic potential of ZnO NPs greatly depends on the integrity of the *TP53* gene, our findings speak in favour of exposure to ZnO NPs as a possible cancer risk factor.

Our approach based on the separation of two lymphocyte populations by density at treatment concentrations above 2.5 μg mL^{-1} and determination of intracellular Zn^{2+} with DPASV and HR-ICPMS showed that there was a significant difference in the uptake rate of ZnO NPs between lymphocytes. Gilbert et al. (41) have already evidenced that ZnO NPs enter cells undissolved. Particles are taken up through endocytosis, primarily via caveolae, and end up in intracellular vesicles (42). Once ZnO enters the cell, it tends to dissolve in aqueous media and convert to its biologically active form Zn^{2+} (43). Unlike caveolae, lysosomes contain zinc only in its ionic form, most likely due to their acidic content, which facilitates the dissolution of ZnO. Cytosolic zinc mostly binds to metalloproteins. Another route for Zn^{2+} uptake from extracellular environment to the cytosol is mediated by Zrt/Irt-like transmembrane proteins (44).

Our regression analysis has shown a strong correlation between ZnO concentrations and intracellular Zn^{2+} levels, especially at concentrations above 5 μg mL^{-1}. Differences in intracellular Zn^{2+} levels resulted in the separation of the lymphocytes by density, which allowed us to separately study the toxic effects in low and high-density populations.

This approach provided additional statistical power to the correlation analysis, whose aim was to test the relation between primary DNA lesions, loss of *TP53* integrity and heterozigocity, and intracellular Zn^{2+} concentrations. Differences in zinc accumulation between cultured cells of the same population have already been reported by Yoo et al. (45). The authors were reluctant to attribute them to the variations in molecular mechanisms involved in the endocytosis of NPs or to transmembrane zinc transporters but rather to the differences in relative surface charge of the nanoparticles. Cells take up positively charged ZnO NPs more efficiently. This explanation, however, does not apply for our study, because all our lymphocytes were exposed to the same nanoparticles and the ratio of positively charged particles should not vary within one culture. The differentiation rather suggests that there are differences in accumulation capacity between lymphocytes at ZnO NP concentrations above 2.5 μg mL^{-1}. As already mentioned, there are several pathways of Zn uptake in the cell, but there is a single way out: via the Zn^{2+}/H^{+} transporter ZnT-1. Yu et al. (46) reported that in human lung epithelial cells intracellular accumulation plateaued at ZnO levels ten times higher than used in our study due to the saturation of the uptake mechanisms. Our results suggest that high-density lymphocytes accumulated higher intracellular Zn^{2+} content with increasing concentrations of ZnO NPs. This finding suggests that mechanisms responsible for Zn^{2+} extrusion get saturated as early as 2.5 μg mL^{-1}, judging by significantly higher intracellular zinc concentrations compared to corresponding low-density lymphocytes (Figure 3).

The value of the comet assay in genotoxicity evaluation of materials with unknown biocompatibility was previously confirmed by Galić et al. (47). The three main parameters most commonly used to quantify DNA damage in the comet assay are the tail length, tail intensity, and tail moment (48). In our study, we assessed both tail length and tail intensity, and the obtained results suggest that they both adequately reflected the level of primary DNA damage. However, many literature sources consider tail intensity as more sensitive, especially at intense genotoxic events when the tail length reaches its maximum and plateaus (49). If ZnO can induce biologically significant primary DNA lesions that would become mutations or chromosome aberrations, tail intensity should exhibit a higher correlation to intracellular Zn^{2+} than tail length. We, however, observed the opposite. Tail length and *TP53* fragmentation correlated with intracellular Zn concentrations, while tail intensity did not. Even so, all highly depended on the migration of the DNA in the electric field during electrophoresis. The only endpoint that did not depend on electrophoresis was the deletion of *TP53*. It also did not significantly correlate either with ZnO NPs or Zn^{2+}.

All things considered, this study has not clarified the issue of the applicability of the comet assay as a widely used technique for assessing the risk of novel nanomaterials. As discussed earlier, ZnO NPs dissociate within the cell, which results in an increase in free intracellular Zn^{2+}. This ionic form of zinc is responsible for the observed adverse effects of ZnO in the cells. As a negatively charged macromolecule, DNA is an ideal target to released Zn^{2+}. These interactions may result in various types of primary DNA damage that are converted by alkaline electrophoresis into additional DNA breaks, which can be visualised and measured with the comet assay. Therefore, understanding Zn^{2+}/DNA interactions and their behaviour in the electric field is crucial for accurate interpretation of the obtained results.

The biological relevance of the obtained results strongly depends on accurate interpretation of the comet assays. In the electric field, denaturated DNA migrates toward the positively charged anode, while complexed Zn^{2+} would

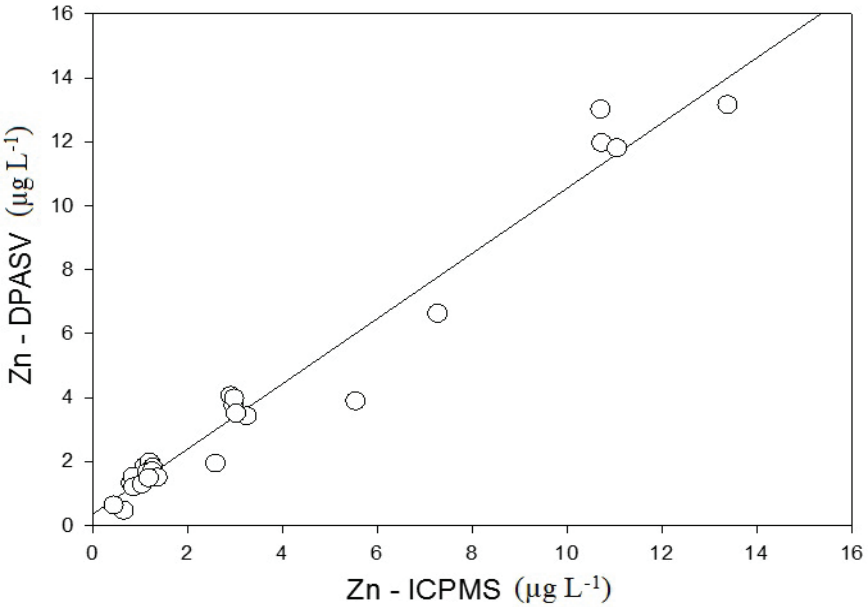

Figure 4 *Comparison of Zn^{2+} concentrations measured with the differential pulse anodic stripping voltammetry (DPASV) and high resolution inductively plasma mass spectrometry (HR-ICMS)*

migrate to the negatively charged cathode. The question remains whether and how complexed Zn^{2+} ions interfere with the ability of damaged DNA to migrate. Does the observed genotoxicity originate from biological interaction between Zn^{2+} and DNA *in situ* or is it an artefact resulting from the assay's limitations? Would complexed Zn^{2+} impair gene expression and stability *in situ*, or is it a consequence of exposing the complexed DNA to the electric field when Zn^{2+} induces strand breaks? It is difficult to answer this question, considering that most studies reported positive results of the alkaline comet assay but did not find oxidative DNA damage following exposure to NPs. As previous studies point, there are discrepancies between the endpoints that depend on comet assay electrophoresis and classical cytogenetic biomarkers (12). In designing protocols for the risk assessment of NP interactions with biological systems we should be aware of the concerns raised by Karlsson (12) and Doak et al. (50) that NPs may interfere with the comet assay outcomes. In spite of these limitations, our study has shown that combining electrochemical with genotoxicity methods can help to evaluate the cyto/genotoxicity of ZnO NPs, but further studies are needed to elucidate their toxicity profile.

Acknowledgements

The work was financed by the Institute for Medical Research and Occupational Health (grant No. 310).

REFERENCES

1. Maynard AD. Challenges in nanoparticle risk assessment. In: Ramachandran G, editor. Assessing nanoparticle risks to human health. 1st ed. Oxford: Elsevier Inc.; 2011. p. 1-19.
2. Kononenko V, Narat M, Drobne D. Nanoparticle interaction with the immue system. Arh Hig Rada Toksikol 2015;66:97-108. doi: 10.1515/aiht-2015-66-2582
3. Shi LE, Li ZH, Zheng W, Zhao YF, Jin YF, Tang ZX. Synthesis, antibacterial activity, antibacterial mechanism and food applications of ZnO nanoparticles: a review. Food Addit Contam Part A Chem Anal Control Expo Risk Assess 2014;31:173-86. doi: 10.1080/19440049.2013.865147
4. Espitia PJP, de Fátima Ferreira Soares N, dos Reis Coimbra JS, de Andrade NJ, Cruz RS, Medeiros EAA. Zinc oxide nanoparticles: synthesis, antimicrobial activity and food packaging applications. Food Bioproc Technol 2012;5:1447-64. doi: 10.1007/s11947-012-0797-6
5. Heng BC, Zhao X, Tan EC, Khamis N, Assodani A, Xiong S, Ruedl C, Ng KW, Loo JS. Evaluation of the cytotoxic and inflammatory potential of differentially shaped zinc oxide nanoparticles. Arch Toxicol 2011;85:1517-28. doi: 10.1007/s00204-011-0722-1
6. Sharma V, Anderson D, Dhawan A. Zinc oxide nanoparticles induce oxidative DNA damage and ROS-triggered mitochondria mediated apoptosis in human liver cells (HepG2). Apoptosis 2012;17:852-70. doi: 10.1007/s10495-012-0705-6
7. Sun J, Wang S, Zhao D, Hun FH, Weng L, Liu H. Cytotoxicity, permeability, and inflammation of metal oxide nanoparticles in human cardiac microvascular endothelial cells: cytotoxicity, permeability, and inflammation of metal oxide nanoparticles. Cell Biol Toxicol 2011;27:333-42. doi: 10.1007/s10565-011-9191-9
8. Pujalté I, Passagne I, Brouillaud B, Treguer M, Durand E, Ohayon-Courtes C, L'Azou B. Cytotoxicity and oxidative stress induced by different metallic nanoparticles on human kidney cells. Part Fibre Toxicol 2011;8:10. doi: 10.1186/1743-8977-8-10
9. Ma-Hock L, Burkhardt S, Strauss V, Gamer AO, Wiench K, Landsiedel R. Inhalation toxicity of nano-scale zinc oxide in comparison with pigmentary zinc oxide using short-term inhalation test protocol. Naunyn-Schmiedeberg's Arch Pharmacol 2008;377(Suppl 1):72.
10. Wang B, Feng W, Wang M, Wang T, Gu Y, Zhu M, Ouyang H, Shi J, Zhang F, Zhao Y, Chai Z, Wang H, Wang J. Acute toxicological impact of nano- and submicro-scaled zinc oxide powder on healthy adult mice. J Nanopart Res 2008;10:263-76. doi: 10.1007/s11051-007-9245-3
11. Zhao X, Wang S, Wu Y, You H, Lv L. Acute ZnO nanoparticles exposure induces developmental toxicity, oxidative stress and DNA damage in embryo-larval zebrafish. Aquat Toxicol 2013;136-137:49-59. doi: 10.1016/j.aquatox.2013.03.019
12. Karlsson HL. The comet assay in nanotoxicology research. Anal Bioanal Chem 2010;398:651-66. doi: 10.1007/s00216-010-3977-0
13. Magdolenova Z, Collins A, Kumar A, Dhawan A, Stone V, Dusinska M. Mechanisms of genotoxicity. A review of *in vitro* and *in vivo* studies with engineered nanoparticles. Nanotoxicology 2014;8:233-78. doi: 10.3109/17435390.2013.773464
14. Reddy KM, Feris K, Bell J, Wingett DG, Hanley C, Punnoose A. Selective toxicity of zinc oxide nanoparticles to prokaryotic and eukaryotic systems. Appl Phys Lett 2007;90:2139021-3. doi: 10.1063/1.2742324
15. Di Virgilio AL, Reigosa M, Arnal PM, Fernandez Lorenzo de Mele M. Comparative study of the cytotoxic and genotoxic effects of titanium oxide and aluminium oxide nanoparticles in Chinese hamster ovary (CHO-K1) cells. J Hazard Mater 2010;177:711-8. doi: 10.1016/j.jhazmat.2009.12.089
16. Yee KS, Vousden KH. Complicating the complexity of p53. Carcinogenesis 2005;26:1317-22. doi: 10.1093/carcin/bgi122
17. Kim YH, Fazlollahi F, Kennedy IM, Yacobi NR, Hamm-Alvarez SF, Borok Z, Kim KJ, Crandall ED. Alveolar epithelial cell injury due to zinc oxide nanoparticle exposure. Am J Respir Crit Care Med 2010;182:1398-409. doi: 10.1164/rccm.201002-0185OC
18. Compton RG, Banks CE. Understanding Voltammetry. 2nd ed. London: Imperial College Press; 2011.
19. Bihari P, Vippola M, Schultes S, Praetner M, Khandoga AG, Reichel CA, Coester C, Tuomi T, Rehberg M, Krombach F. Optimized dispersion of nanoparticles for biological *in vitro* and *in vivo* studies. Part Fibre Toxicol 2008;5:14. doi: 10.1186/1743-8977-5-14
20. Mladinić M, Želježić D, Shaposhnikov SA, Collins AR. The use of FISH-comet to detect c-Myc and TP 53 damage in extended-term lymphocyte cultures treated with terbuthylazine and carbofuran. Toxicol Lett 2012;211:62-9. doi: 10.1016/j.toxlet.2012.03.001
21. Duke RC, Cohen JJ. Morphological and biochemical assays of apoptosis. In: Janssen K, editor. Current protocols in

immunology. New York (NY): John Willey and Sons; 1992. p. 3.17.1-16.
22. Singh NP, McCoy MT, Tice RR, Schneider EL. A simple technique for quantitation of low levels of DNA damage in individual cells. Exp Cell Res 1988;175:184-91. doi: 10.1016/0014-4827(88)90265-0
23. Mladinić M, Želježić D. Modification of comet-FISH technique by using temperature instead of chemical denaturation. MethodsX 2014;1:162-7. doi: 10.1016/j.mex.2014.08.010
24. Vukosav P, Mlakar M, Cukrov N, Kwokal Ž, Pižeta I, Pavlus N, Špoljarić I, Vurnek, M, Brozinčević A, Omanović D. Heavy metal contents in water, sediment and fish in a karst aquatic ecosystem of the Plitvice Lakes National Park (Croatia). Environ Sci Pollut Res Int 2014;21:3826-39. doi: 10.1007/s11356-013-2377-3
25. Cobelo-Garcia A, Santos-Echeandia J, Lopez-Sanchez DE, Almecija C, Omanović, D. Improving the voltammetric quantification of ill-defined peaks using second derivative signal transformation: example of the determination of platinum in water and sediments. Anal Chem 2014;86:2308-13. doi: 10.1021/ac403558y
26. Lenoble V, Omanović D, Garnier C, Mounier S, Donlagić N, Le Poupon C, Pižeta I. Distribution and chemical speciation of arsenic and heavy metals in highly contaminated waters used for health care purposes (Srebrenica, Bosnia and Herzegovina). Sci Total Environ 2013;443:420-8. doi: 10.1016/j.scitotenv.2012.10.002
27. Ivask A, Juganson K, Bondarenko O, Mortimer M, Aruoja V, Kasemets K, Blinova I, Heinlaan M, Slaveykova V, Kahru A. Mechanisms of toxic action of Ag, ZnO and CuO nanoparticles to selected ecotoxicological test organisms and mammalian cells *in vitro*: A comparative review. Nanotoxicology 2014;8:57-71. doi: 10.3109/17435390.2013.855831
28. Jignesh S, Vineeta K, Abhay S, Vilasrao K. Analytical methods for estimation of metals. Int J Res Pharm Chem 2012;2:146-63.
29. Guo D, Bi H, Wu Q, Wang D, Cui Y. Zinc oxide nanoparticles induce rat retinal ganglion cell damage through bcl-2, caspase-9 and caspase-12 pathways. J Nanosci Nanotechnol 2013;13:3769-777. doi: 10.1166/jnn.2013.7169
30. Mu Q, David CA, Galceran J, Rey-Castro C, Krzemiński Ł, Wallace R, Bamiduro F, Milne SJ, Hondow NS, Brydson R, Vizcay-Barrena G, Routledge MN, Jeuken LJ, Brown AP. Systematic investigation of the physicochemical factors that contribute to the toxicity of ZnO nanoparticles. Chem Res Toxicol 2014;27:558-67. doi: 10.1021/tx4004243
31. Demir E, Akça H, Kaya B, Burgucu D, Tokgün O, Turna F, Aksakal S, Vales G, Creus A, Marcos R. Zinc oxide nanoparticles: Genotoxicity, interactions with UV-light and cell-transforming potential. J Hazard Mater 2014;264:420-9. doi: 10.1016/j.jhazmat.2013.11.043
32. Sharma V, Shukla RK, Saxena N, Parmar D, Das M, Dhawan A. DNA damaging potential of zinc oxide nanoparticles in human epidermal cells. Toxicol Lett 2009;185:211-8. doi: 10.1016/j.toxlet.2009.01.008
33. Osman IF, Baumgartner A, Cemeli E, Fletcher JN, Anderson D. Genotoxicity and cytotoxicity of zinc oxide and titanium dioxide in HEp-2 cells. Nanomedicine 2010:5:1193-203. doi: 10.2217/nnm.10.52
34. Horinouchi M, Arimoto-Kobayashi S. Photomicronucleus assay of phototoxic and pseudophotoclastogenic chemicals in human keratinocyte NCTC2544 cells. Mutat Res 2011;723:43-50. doi: 10.1016/j.mrgentox.2011.04.005
35. Sharma V, Singh SK, Anderson D, Tobin DJ, Dhawan A. Zinc oxide nanoparticle induced genotoxicity in primary human epidermal keratinocytes. J Nanosci Nanotechnol 2011;11:3782-8. doi: 10.1166/jnn.2011.4250
36. Hackenberg S, Scherzed A, Technau A, Kessler M, Froelich K, Ginzkey C, Koehler C, Burghartz M, Hagen R, Kleinsasser N. Cytotoxic, genotoxic and pro-inflammatory effects of zinc oxide nanoparticles in human nasal mucosa cells *in vitro*. Toxicol In Vitro 2011;25:657-63. doi: 10.1016/j.tiv.2011.01.003
37. Sharma V, Anderson D, Dhawan A. Zinc oxide nanoparticles induce oxidative stress and genotoxicity in human liver cells (HepG2). J Biomed Nanotechnol 2011;7:98-9. doi: 10.1166/jbn.2011.1220
38. Guan R, Kang T, Lu F, Zhang Z, Shen H, Liu M. Cytotoxicity, oxidative stress, and genotoxicity in human hepatocyte and embryonic kidney cells exposed to ZnO nanoparticles. Nanosc Res Lett 2012;7:602. doi: 10.1186/1556-276X-7-602
39. Ahamed M, Akhtar MJ, Raja M, Ahmad I, Siddiqui MK, AlSalhi MS, Alrokayan SA. ZnO nanorod-induced apoptosis in human alveolar adenocarcinoma cells via p53, survivin and bax/bcl-2 pathways: role of oxidative stress. Nanomedicine 2011;7:904-13. doi: 10.1016/j.nano.2011.04.011
40. Ng KW, Khoo SP, Heng BC, Setyawati MI, Tan EC, Zhao X, Xiong S, Fang W, Leong DT, Loo JS. The role of the tumor suppressor p53 pathway in the cellular DNA damage response to zinc oxide nanoparticles. Biomaterials 2011;32:8218-25. doi: 10.1016/j.biomaterials.2011.07.036
41. Gilbert B, Fakra SC, Xia T, Pokhrel S, Mädler L, Nel AE. The fate of ZnO nanoparticles administered to human bronchial epithelial cells. ACS Nano 2012;6:4921-30. doi: 10.1021/nn300425a
42. Roy R, Parashar V, Chauhan L, Shanker R, Das M, Tripathi A, Dwivedi PD. Mechanism of uptake of ZnO nanoparticles and inflammatory responses in macrophages require PI3K mediated MAPKs signaling. Toxicol In Vitro 2014;28:457-67. doi: 10.1016/j.tiv.2013.12.004
43. Moos PJ, Chung K, Woessner D, Honeggar M, Cutler NS, Veranth JM. ZnO particulate matter requires cell contact for toxicity in human colon cancer cells. Chemical research in toxicology 2010;23:733-9. doi: 10.1021/tx900203v
44. Xia T, Kovochich M, Liong M, Mädler L, Gilbert B, Shi H, Yeh JI, Zink JI, Nel AE. Comparison of the mechanism of toxicity of zinc oxide and cerium oxide nanoparticles based on dissolution and oxidative stress properties. ACS nano 2008;2:2121-34. doi: 10.1021/nn800511k
45. Yoo HJ, Yoon TH. Flow cytometric assessment of reactive oxygen species generations that are directly telated to cellular ZnO nanoparticle uptake. J Nanosci Nanotechnol 2014;14:5395-401. doi: 10.1166/jnn.2014.8733
46. Yu J, Baek M, Chung H, Choi S. Effects of physicochemical properties of zinc oxide nanoparticles on cellular uptake. J Phys Conf Ser 2011;304:012007. doi: 10.1088/1742-6596/304/1/012007
47. Galić E, Tadin A, Galić N, Kašuba V, Mladinić M, Rozgaj R, Biočina-Lukenda D, Galić I, Želježić D. Micronucleus, alkaline, and human 8-oxoguanine glycosylase 1 modified comet assays evaluation of glass-ionomer cements - *in vitro*. Arh Hig Rada Toksikol 2014;65:179-88. doi: 10.2478/10004-1254-65-2014-2392

48. Rojas E, Lopez MC, Valverde M. Single cell electrophoresis assay: methodology and applications. J Chrom B Biomed Sci Appl 1999;722:225-54. doi: 10.1016/S0378-4347(98)00313-2
49. Collins AR, Oscoz AA, Brunborg G, Gaivao I, Giovannelli L, Kruszewski M, Smith CC, Stetina R. The comet assay: topical issues. Mutagenesis 2008;23:143-51. doi: 10.1093/mutage/gem051
50. Doak S, Griffiths S, Manshian B, Singh N, Williams P, Brown A, Jenkins G. Confounding experimental considerations in nanogenotoxicology. Mutagenesis 2009;24:285-93. doi: 10.1093/mutage/gep010

Alternativni pristup mjerenju koncentracije nanočestica ZnO u kulturama humanih limfocita - spoj elektrokemije i testova genotoksičnosti

S naglim porastom primjene nanočestica raste i mogućnost njihova štetna djelovanja u ljudi. Nanočestice cinkova oksida najčešći su oblik nanomaterijala u potrošačkim proizvodima i lijekovima. Nekoliko je istraživanja već upozorilo na probleme vezane uz njihovu sigurnu primjenu. Cilj je ovoga istraživanja bio utvrditi pri kojim razinama nanočestice ZnO počinju štetno citogenetski djelovati na humane limfocite i time otvoriti pitanje utvrđivanja graničnih razina za sigurnu primjenu nanočestica ZnO u ljudi. Stoga smo istražili genotoksične učinke niskih koncentracija nanočestica ZnO (1,0; 2,5; 5 i 7,5 μg mL^{-1}) izloživši kulture humanih limfocita njihovu djelovanju tijekom 14 dana. Uz to smo izmjerili razlikuju li se limfociti niske gustoće od onih visoke gustoće u sposobnosti akumuliranja nanočestica ZnO pri istim eksperimentalnim uvjetima. Primarno oštećenje DNA (izmjereno alkalnim komet-testom) povećalo se s rastom koncentracije nanočestica u limfocitima koje nismo razdvojili po gustoći te u limfocitima visoke gustoće. Slično smo povećanje zamijetili s fragmentacijom tumorskoga supresorskoga gena TP53 (izmjereno komet-FISH testom). Nakupljanje Zn^{2+} iona u stanicama bilo je značajno samo kod primjene dviju najviših koncentracija nanočestica ZnO, bez obzira na gustoću limfocita. Osim toga, limfociti visoke gustoće iskazali su i značajno više razine unutarstaničnoga Zn^{2+} od limfocita niske gustoće. Naši rezultati upozoravaju na to da se izlaganjem razinama nanočestica ZnO višima od 5 μg mL^{-1} značajno povisuju razine Zn^{2+} u limfocitima te se povećava oštećenje tih stanica i njihova genoma.

KLJUČNE RIJEČI: *komet-FISH test,* in vitro*; primarno oštećenje DNA;* TP53*; voltametrija*